

Two-dimensional water seepage monitoring in concrete structures using smart aggregates

Dujian Zou^a, Weijie Li^b, Tiejun Liu^{*} and Jun Teng^c

Shenzhen Key Laboratory of Urban and Civil Engineering for Disaster Prevention and Mitigation, Shenzhen Graduate School, Harbin Institute of Technology, Shenzhen 518055, People's Republic of China

(Received January 25, 2018, Revised March 20, 2018, Accepted March 23, 2018)

Abstract. The presence of water inside concrete structures is an essential condition for the deterioration of the structures. The free water in the concrete pores and micro-cracks is the culprit for the durability related problems, such as alkali-aggregate reaction, carbonation, freeze-thaw damage, and corrosion of steel reinforcement. To ensure the integrity and safe operation of the concrete structures, it is very important to monitor water seepage inside the concrete. This paper presents the experimental investigation of water seepage monitoring in a concrete slab using piezoelectric-based smart aggregates. In the experimental setup, an 800 mm × 800 mm × 100 mm concrete slab was fabricated with 15 SAs distributed inside the slab. The water seepage process was monitored through interrogating the SA pairs. In each SA pair, one SA was used as actuator to emit harmonic sine wave, and the other was used as sensor to receive the transmitted stress wave. The amplitudes of the received signals were able to indicate the water seepage process inside the concrete slab.

Keywords: concrete structures; water seepage monitoring; smart aggregates

1. Introduction

Concrete is the most widely used construction material in our physical world. Under the conditions of complicated loads and hostile environments, the durability of the concrete structures is significantly compromised. The presence of water or moisture inside concrete structures is an essential condition for the degradation of the structures (Richardson 2003). The strength, shrinkage and creep of concrete are closely related to the water content inside the concrete. The free water in the concrete pores is responsible for major durability issues, such as alkali-aggregate reaction, carbonation, freeze-thaw damage, and corrosion of steel reinforcement. To ensure the integrity and safe operation of the concrete structures, several kinds of structural monitoring methods has been proposed and widely used (Yi *et al.* 2011, 2013a). It is very important to monitor water seepage inside the concrete.

The conventional methods to measure water content in concrete are slice weighing method

*Corresponding author, Professor, E-mail: liutiejun@hit.edu.cn

^a Ph.D., E-mail: zoudujian@163.com

^b Post-doctoral Researcher, E-mail: wli27@uh.edu

^c Professor, E-mail: tengj@hit.edu.cn

(Goual *et al.* 2000), nuclear magnetic resonance (Leech *et al.* 2003), gamma-ray spectrometer (Quenard and Sallee 1988), and thermal conductivity (Saare and Jansson 1961). These methods achieved the water content measurement in certain aspects, but were limited in others. The slice weighing method is destructive and the process is complicated, which requires a lot of manpower. The nuclear magnetic resonance and gamma-ray spectrometer pose potential hazard to the personnel. The thermal conductivity method is sensitive but the measurement limited to small region. These conventional methods are generally not suitable for real time monitoring of water in concrete. With the advances in smart materials and sensing technologies, various types of new sensors have been developed to monitor the water and internal relative humidity in concrete. Yeo *et al.* (2005) fabricated a fiber-optic-based humidity sensor through coating fiber Bragg grating (FBG) with a moisture-sensitive polymer (Yeo *et al.* 2005). The relative humidity is obtained by the polymer coating swelling induced wavelength shift of the FBG. Shukla *et al.* (2004) devised a humidity sensor by coating the water-absorbing nanosize MgO on the U-shaped optical fiber (Shukla *et al.* 2004). The output optical power is indicative of the humidity surrounding the sensing element. Norris proposed the use of micro-electromechanical systems (MEMS) to measure temperature and internal relative humidity (RH) using micro-cantilever beams and moisture-sensitive thin polymer (Norris *et al.* 2008). The MEMS outputs is able to reflect the moisture content and temperature effectively. Ho *et al.* designed a FBG liquid water sensor by integrating the superabsorbent polymer and FBG strain sensor (Ho *et al.* 2013). The swelling of superabsorbent polymer exert strain on the FBG and thus the presence of water inside concrete can be detected. These new water and humidity sensors are still in their infancy, which requires further laboratory testing and calibration before they can be applied in practical engineering.

The quick development in smart materials and sensing technology expands the monitoring methods greatly (Yi and Li 2012, Yi *et al.* 2013b). Smart aggregate (SA), which is fabricated by sandwiching a lead zirconate titanate (PZT) patch between two marble blocks, has emerged as a new structural health monitoring tool for concrete structures (Song *et al.* 2008, Yan *et al.* 2009, Liao *et al.* 2011, Li *et al.* 2016). Essentially, the SA has the same size as the aggregate of concrete, which can be conveniently embedded inside concrete for damage interrogation. The SAs can act as actuators to generate signals and sensors to receive signals. Extensive experimental studies have been conducted during the past several years using SAs for health monitoring of concrete structures. For example, the SAs were used to detect debonding damage (Qin *et al.* 2015, Jiang *et al.* 2017, Xu *et al.* 2017), cracks (Dumoulin *et al.* 2014, Feng *et al.* 2015, Kong *et al.* 2015, Feng *et al.* 2016), and concrete strength gain (Gu *et al.* 2006, Kong *et al.* 2013). These studies were mostly focused on the monitoring of loading states and damage conditions of concrete structures, while the topics on the monitoring of water seepage in concrete are rarely reported. Liu *et al.* (2013) firstly explored the seepage monitoring in concrete structures using SAs (Liu *et al.* 2013). The energy-based indices were used to indicate the depth of water seepage. Subsequently, relation between the travel time of the harmonic stress wave and water seepage depth was explored (Zou *et al.* 2014).

Our previous investigations (Liu *et al.* 2013, Zou *et al.* 2014) were preliminary and the water seepage path was one-dimensional. As a continuation of our previous work, this paper extended the complexity of water seepage monitoring and explored the water seepage characteristics in two-dimensional setup. An 800 mm × 800 mm × 100 mm concrete slab was fabricated with 15 SAs distributed inside the slab. The slab was subjected to water seepage and the SAs were used to interrogate water seepage information.

2. Principle of piezoelectric-based smart aggregates

Piezoelectricity describes the phenomenon that a piezoelectric material is able to convert mechanical energy into electrical energy and vice versa (Tressler *et al.* 1998). In direct piezoelectricity, electric charges are produced when stress is applied. In inverse piezoelectricity, the piezoelectric material deforms when electrical field is applied. Thus, the piezoelectric material can be used as sensor based on the direct piezoelectric effect and as actuator based on the inverse piezoelectric effect. The lead zirconate titanate (PZT) is one type of piezoelectric ceramics that are widely used for structural health monitoring of various structures (Zou *et al.* 2014, Zou *et al.* 2015, Du *et al.* 2017, Liu *et al.* 2017, Zou *et al.* 2017).

According to compact matrix notation (Lin and Yuan 2001), the coupled electromechanical constitutive equations of a linear piezoelectric material can be described as

$$\begin{bmatrix} D \\ S \end{bmatrix} = \begin{bmatrix} \varepsilon^T & d \\ d^T & s^E \end{bmatrix} \begin{bmatrix} E \\ T \end{bmatrix} \quad (1)$$

where D and E are the electric displacement and electric field respectively. S and T are the mechanical strain and stress. d , ε^T and s^E are the piezoelectric strain constant, dielectric permittivity and compliance constant, respectively. The superscripts E and T indicate that the values of the constant stress respectively.

The SA was fabricated by sandwiching a PZT patch between two marble blocks with epoxy (Song *et al.* 2008), as shown in Fig. 1. The PZT patch has the size of 15 mm × 15 mm with a thickness of 0.3 mm. The size of the marble block is 25 mm × 25 mm × 12 mm and the thickness of the epoxy layer is 1 mm. Thus the SA has the size of 25 mm × 25 mm × 25 mm. The PZT used is PZT-5H, whose properties are listed in Table 1. The marble blocks and epoxy protect the fragile PZT patch from external disturbance and water damage. In addition, the structure maximizes the energy transmission between the PZT patch and the test specimen. Since SAs share the same size as aggregates in concrete mix, the embeddability and compatibility between the SAs and the tested structure are guaranteed.

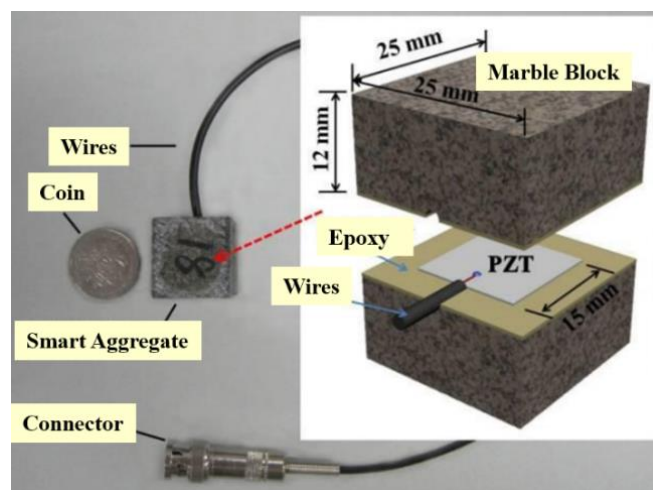


Fig. 1 Photo of the smart aggregate

Table 1 Properties of the PZT patch

Property (unit)	Magnitude
Density (g/cm^3)	7.5
d_{33} (pC N^{-1})	450
Capacitance (pF)	4500
Relative dielectric constant	1600
Electromechanical coupling factor	0.8

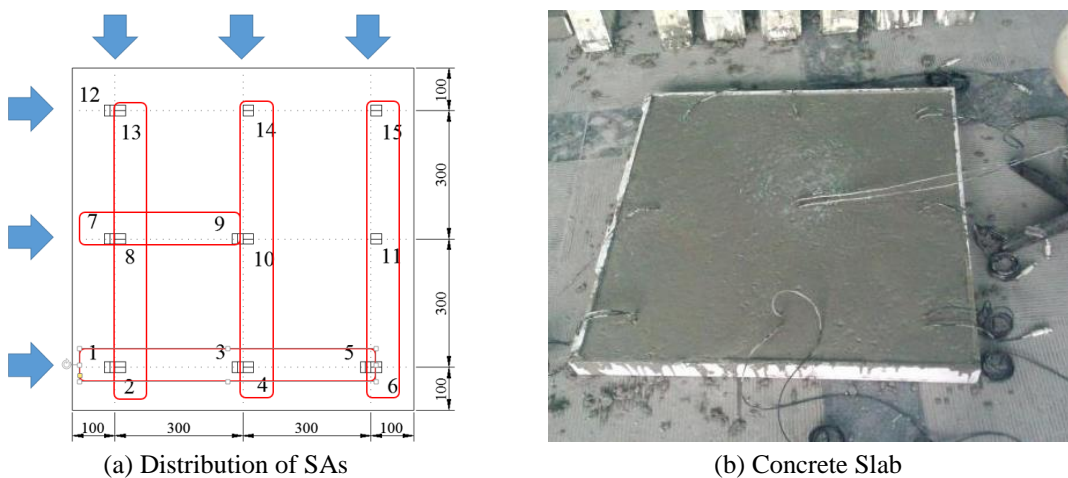


Fig. 2 The fabricated concrete slab

3. Experimental setup of water seepage monitoring using SAs

To study the water seepage characteristics in two-dimensional setting, a concrete slab was fabricated with 15 SAs distributed inside the slab, as shown in Fig. 2. The concrete slab has a dimension of $800 \text{ mm} \times 800 \text{ mm} \times 100 \text{ mm}$. Fig. 2 illustrates the distribution of the SAs, where the SAs are oriented in two different directions. The concrete used is C60 and the mix ratio by weight is cement:sand:stone:water = 1:1.32:2.35:0.33. The concrete slab was cured for 28 days before water seepage monitoring experiments.

In the seepage monitoring experiments, the concrete slab was placed in an oven and dried for 24 hours under 75°C . The specimen was further dried under 105°C until its weight remain unchanged. All other faces of the slab were waxed to prevent water penetration except the two faces marked by arrows in Fig. 2(a). These two faces were designed to allow the water seepage. Subsequently, the specimen was placed in a tank and the water depth was kept at 11 cm, i.e., 1 cm higher than the concrete slab.

The active sensing approach was adopted, in which one SA was used as actuator and the other was used as sensor in the SA pair. The SA pairs were marked with red box in Fig. 2(a). There were 13 pairs of SAs in total. They were 13-8, 13-2, 8-2, 14-10, 14-4, 10-4, 15-11, 15-6, and 11-6 pairs

in vertical direction and 7-9, 1-3, 1-5, and 3-5 pairs in horizontal direction. The instrumentation of the active sensing approach is shown in Fig. 3. The monitoring system consists of waveform generator (33210A, Keysight Technologies), power amplifier (Model 603, Trek, Inc), SA pairs, and oscilloscope (MDO3000, Tektronix, Inc). In the monitoring setup, the waveform generator generates 1 V sine signal. The signals were amplified 100 times by the power amplifier before being fed to the SA actuator. The SA sensor received the signals and they were displayed and stored in the oscilloscope. Four excitation signals were tested, namely, the 5 Hz, 20 Hz, 50 Hz, and 100 Hz sine waves. The water seepage information was interrogated every day on the first ten days, and the interrogation became less frequent until the experiment stopped on the 45th day.

4. Results and discussion

Prior to performing the water seepage monitoring of the concrete slab, the amplitudes of the received signals were calibrated (see Table 2). Fig. 4 shows the representative results of SA pairs (7-9, 13-8, 14-4) under different excitation frequency. In the legend of the figure, notation 7→9 denotes SA No. 7 is actuator and SA No. 9 is sensor. The amplitude here is the amplitude of the signal received by the sensor. It can be seen, for the same SA pair, the amplitude of the received signal decreases with the increase of excitation frequency. The high frequency signal is more easily attenuated in concrete material. However, different pair of SA shows different level of amplitude. There are two main reasons for such phenomenon. First, the propagation path of the stress wave is not the same for each SA pair. Second, the SAs were not well-aligned during the pouring of the concrete. In an ideal situation, the central axes of the SA pair should be perfectly aligned, which permits the strongest signal reception.

In order to compare the results clearly, the SA pairs with the same d_{33} direction were plotted in one graph. The red boxes in Fig. 2(a) show such SA pairs. They are five groups of SA pairs, including 13-8-2, 14-10-4, 15-11-6, 7-9, and 1-3-5. The SA pairs 14-10-4 were damaged during the oven dry process, and their signals showed abnormality. The wire for SA No. 1 was broken during the concrete slab fabrication process. Therefore, only the results of SA pairs 13-8-2, 15-11-6, 7-9, and 3-5 were presented.

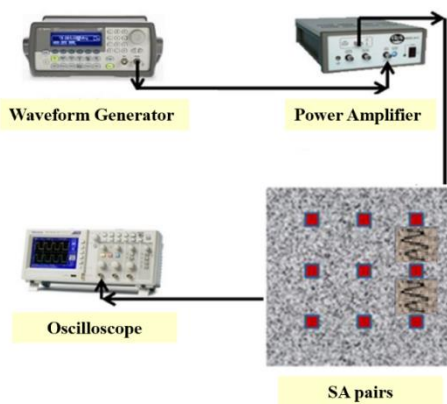


Fig. 3 The instrumentation of the active sensing approach

Table 2 Amplitudes of SA pairs under different excitation frequency

SA pair	5 Hz	20 Hz	50 Hz	100 Hz
13→8	11.4	5.28	2.18	0.536
13→2	0.040	0.038	0.034	0.024
8→2	0.492	0.508	0.46	0.352
13←8	12.6	6.16	2.84	0.792
13←2	0.011	0.017	0.019	0.021
8←2	0.248	0.38	0.392	0.3
14→10	12.1	5.76	2.3	0.464
14→4	0.68	0.464	0.312	0.142
10→4	0.88	0.584	0.372	0.158
14←10	7.04	3.88	1.64	0.368
14←4	0.576	0.348	0.228	0.11
10←4	0.38	0.216	0.124	0.054
15→11	0.48	0.216	0.107	0.037
15→6	1.46	0.888	0.472	0.16
11→6	0.456	0.186	0.087	0.0324
15←11	0.266	0.148	0.074	0.025
15←6	0.848	0.516	0.268	0.082
11←6	0.464	0.168	0.071	0.026

The received signal amplitudes of different SA pairs versus water seepage duration at 5 Hz excitation frequency are shown in Fig. 5. In general, the signals showed an abrupt increase at the initial phase of the water seepage experiments and then the signals were gradually stabilized.

The received signal amplitudes of SA pair 13-8-2 are shown in Fig. 5(a). The amplitude of SA pair 13-8 showed the earliest increase since it was located right at the water seepage entrance. The amplitude of SA pair 13-8 increased suddenly on the first day of water seepage experiment and reached the peak value on the third day. The SA pairs 13-2 and 8-2 did not show an increasing trend until the 10th day, and their amplitudes were peaked on around 19th day. The time-histories of these amplitudes indicate the water seepage process inside the concrete slab.

Similarly, the received signal amplitudes of SA pair 15-11-6 are shown in Fig 5(b). The amplitudes of SA pairs 15-11 and 15-6 stabilized on the third day of the seepage experiment while those for SA pair 11-6 kept increasing and peaked on the 25th day. As shown in Fig. 5(c), the amplitudes of SA pair 7-9 reached its first peak on the fourth day of the seepage experiment. After that, the amplitude fluctuated and kept rising after the 25th day. As depicted in Fig. 5(d), the amplitudes of SA pair 3-5 showed the most retarded action to the water seepage. The amplitude did not show obvious increase until the 19th day. This is because SA pair 3-5 located the furthest away from the seepage entrance.

The reason for the sudden increase in the signal amplitude can be explained as follows. The liquid water fills the pores and micro-cracks of the concrete, making it easier for the stress wave to propagate. It is well-acknowledged that the presence of pores and micro-cracks deflects and diffracts the stress waves, which significantly attenuates the energy of the stress wave. The liquid

water filled in the pores and cracks reduced the deflection and diffraction mechanisms. Thus, stronger signal can be received during the water seepage process.

Supposed all other environmental variable are kept unchanged, the only variable is the water content inside the concrete. That is, the distribution of water content in the propagation path. In this way, the water seepage process can be identified. Take the results of SA pair 13-8 and 3-5 as examples. The received signal amplitudes of 13-8 showed a sudden increase in the very early stage of the seepage monitoring process, while those for SA pair 3-5 did not show obvious increase until the 19th day. Therefore, the moments of sudden increase in amplitude provide the information of the water seepage process.

The excitation frequencies of 20 Hz, 50 Hz, and 100 Hz were also adopted. The amplitudes of the signals at these frequencies were compared to the amplitudes at 5 Hz in order to obtain amplitude ratio. Fig. 6 shows the representative amplitude ratios of SA pairs 13-5 and 15-11. As can be observed, the amplitudes at these frequencies shared the same increasing trend as those at 5 Hz frequency. In general, the amplitudes decrease with the increase of excitation frequency.

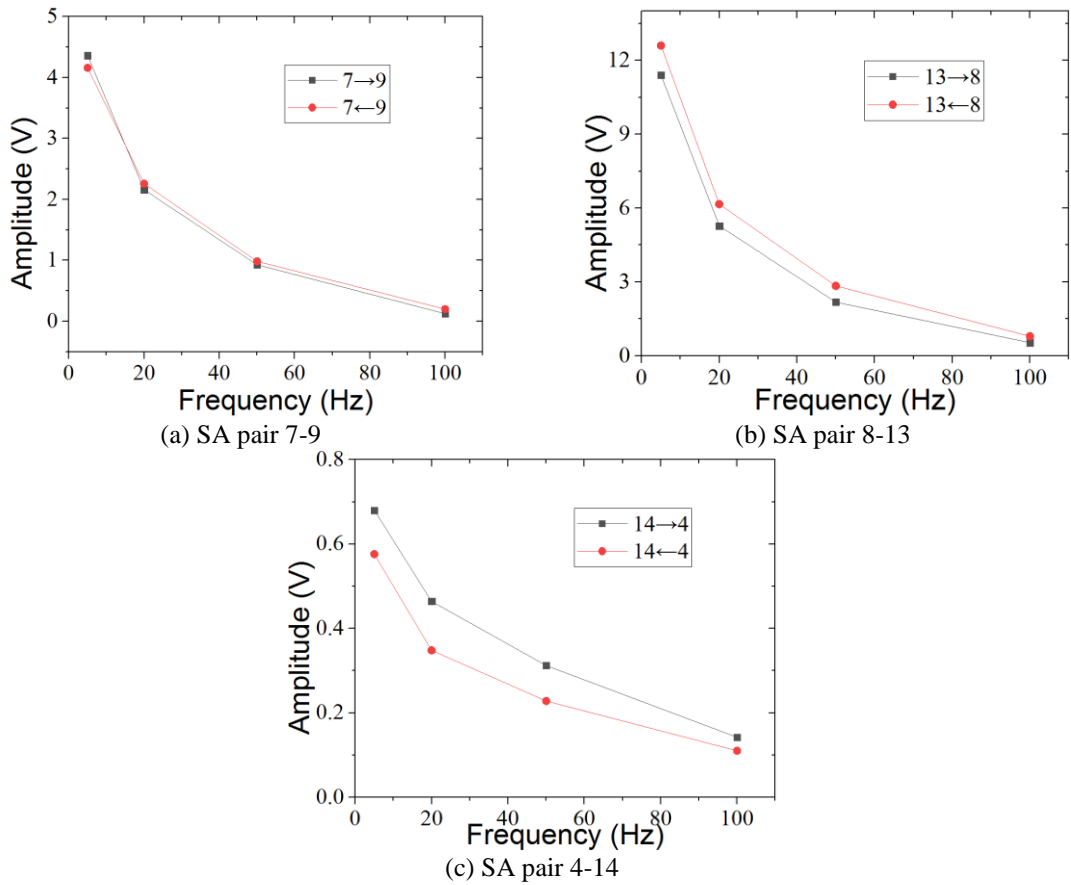


Fig. 4 Received signal amplitudes of SA pairs under different excitation frequency

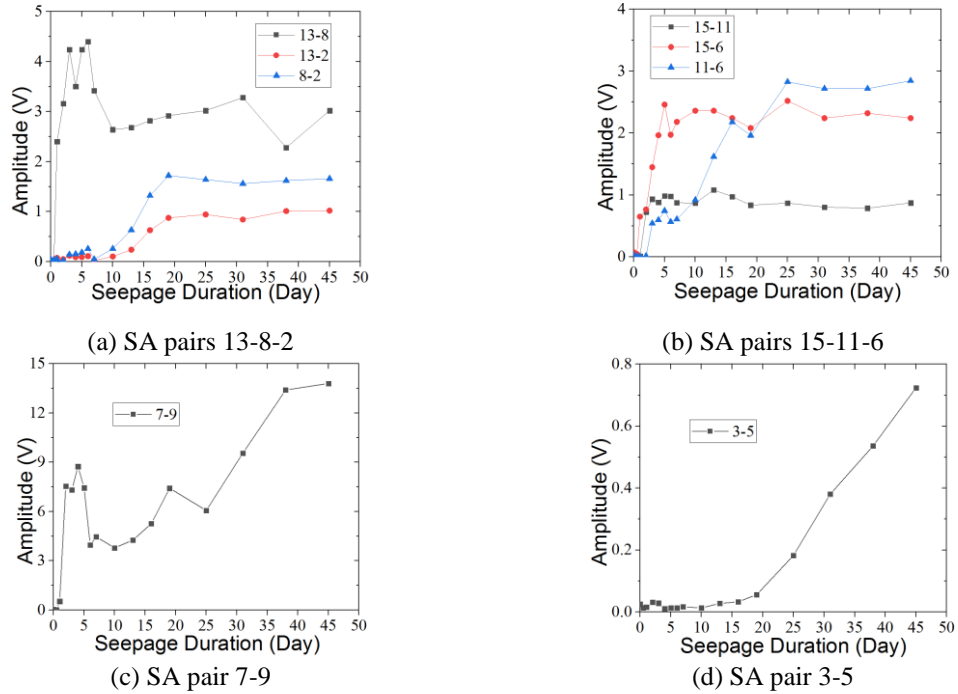


Fig. 5 Received signal amplitudes of different SA pairs versus water seepage duration at 5 Hz excitation frequency

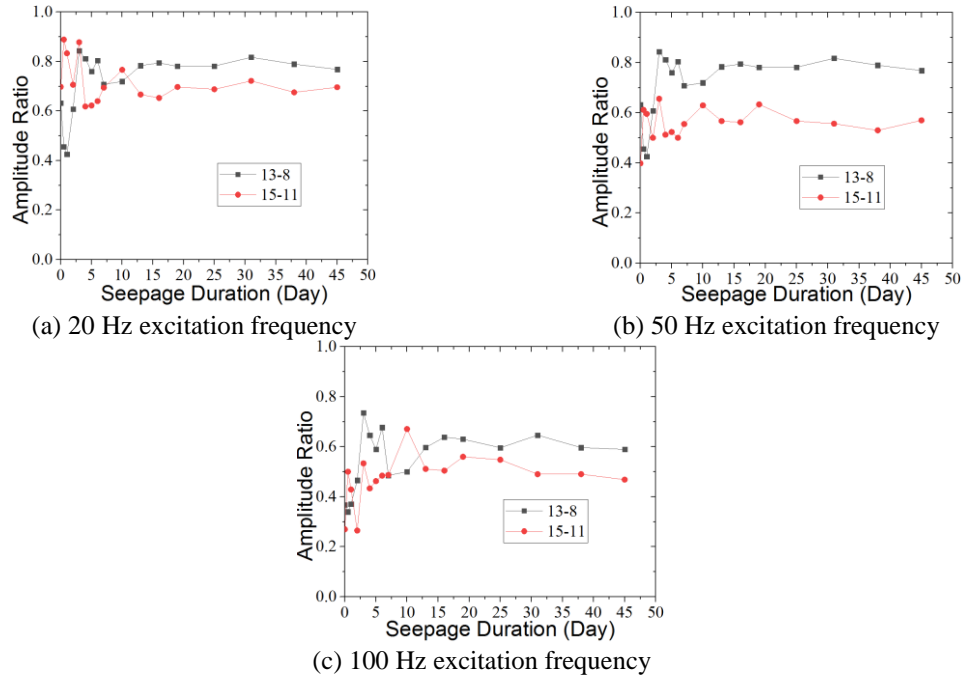


Fig. 6 Representative amplitude ratios

5. Conclusions

In this work, the two-dimensional water seepage monitoring in concrete structures was investigated using the piezoelectric-based smart aggregates. Thereafter, an 800 mm × 800 mm × 100 mm concrete slab was fabricated with 15 SAs distributed inside the slab. The concrete slab was subjected to water seepage experiment and the seepage information was acquired through interrogating the SA pairs. The excitation signal used was sine wave of different frequencies, including 5 Hz, 20 Hz, 50 Hz, and 100 Hz. By analyzing the experimental results, the following conclusions can be made.

- The amplitude of the received signal decreases with increase of the excitation frequency. Therefore, low frequencies are suggested for real world application of the proposed seepage monitoring method.
- The amplitude of the received signal shows an abrupt increase once water is detected along the path of the SA pair. The signal is then gradually stabilized.
- Using a single amplitude index is hard to quantitative assess the water seepage process in concrete. The sudden increase in signal amplitude is more appropriate for early warning for water seepage. For identifying the detail water seepage process in two-dimensional concrete slab, amplitude, wave velocity and fundamental frequency can be combined used to describe water seepage process, which will be discussed in our future study.

Acknowledgments

The research described in this paper was financially supported by the Natural Science Foundation (Grant Nos. 51678200, 51678205), Program of Shenzhen Science and Technology Plan (Grant No. JCYJ20170307150200952), Guangdong Provincial Natural Science Foundation of China (Grant No. 2017A030313259), and Project (GDDCE 16-09) supported by Guangdong Provincial Key Laboratory of Durability for Civil Engineering, Shenzhen University.

References

- Du, C., Zou, D., Liu, T. and Lv, H. (2018), “An exploratory experimental and 3D numerical investigation on the effect of porosity on wave propagation in cement paste”, *Measurement*, **122**, 611-619.
- Dumoulin, C., Karaikos, G., Sener, J.Y. and Deraemaeker, A. (2014), “Online monitoring of cracking in concrete structures using embedded piezoelectric transducers”, *Smart Mater. Struct.*, **23**(11), 115016.
- Feng, Q., Kong, Q., Huo, L. and Song, G. (2015), “Crack detection and leakage monitoring on reinforced concrete pipe”, *Smart Mater. Struct.*, **24**(11), 115020.
- Feng, Q., Kong, Q. and Song, G. (2016), “Damage detection of concrete piles subject to typical damage types based on stress wave measurement using embedded smart aggregates transducers”, *Measurement*, **88**, 345-352.
- Goual, M., Barquin, F.D., Benmalek, M., Bali, A. and Quéneudec, M. (2000), “Estimation of the capillary transport coefficient of Clayey Aerated Concrete using a gravimetric technique”, *Cement Concrete Res.*, **30**(10), 1559-1563.
- Gu, H., Song, G., Dhonde, H., Mo, Y. and Yan, S. (2006), “Concrete early-age strength monitoring using embedded piezoelectric transducers”, *Smart Mater. Struct.*, **15**(6), 1837.
- Ho, S.C.M., Ren, L., Li, H.N. and Song, G. (2013), “A fiber Bragg grating sensor for detection of liquid

- water in concrete structures”, *Smart Mater. Struct.*, **22**(5), 055012.
- Jiang, T., Kong, Q., Patil, D., Luo, Z., Huo, L. and Song, G. (2017), “Detection of debonding between fiber reinforced polymer bar and concrete structure using piezoceramic transducers and wavelet packet analysis”, *IEEE Sen. J.*, **17**(7), 1992-1998.
- Kong, Q., Feng, Q. and Song, G. (2015), “Water presence detection in a concrete crack using smart aggregates”, *J. Smart Nano Mater.*, **6**(3), 149-161.
- Kong, Q., Hou, S., Ji, Q., Mo, Y. and Song, G. (2013), “Very early age concrete hydration characterization monitoring using piezoceramic based smart aggregates”, *Smart Mater. Struct.*, **22**(8), 085025.
- Leech, C., Lockington, D. and Dux, P. (2003), “Unsaturated diffusivity functions for concrete derived from NMR images”, *Mater. Struct.*, **36**(6), 413.
- Li, W., Kong Q., Ho, S.C.M., Mo, Y. and Song, G. (2016), “Feasibility study of using smart aggregates as embedded acoustic emission sensors for health monitoring of concrete structures”, *Smart Mater. Struct.*, **25**(11), 115031.
- Liao, W.I., Wang, J., Song, G., Gu, H., Olmi, C., Mo, Y., Chang, K. and Loh, C. (2011), “Structural health monitoring of concrete columns subjected to seismic excitations using piezoceramic-based sensors”, *Smart Mater. Struct.*, **20**(12), 125015.
- Lin, X. and Yuan, F. (2001), “Diagnostic Lamb waves in an integrated piezoelectric sensor/actuator plate: analytical and experimental studies”, *Smart Mater. Struct.*, **10**(5), 907.
- Liu, T., Huang, Y., Zou, D., Teng, J. and Li, B. (2013), “Exploratory study on water seepage monitoring of concrete structures using piezoceramic based smart aggregates”, *Smart Mater. Struct.*, **22**(6), 065002.
- Liu, T., Zou, D., Du, C. and Wang, Y. (2017), “Influence of axial loads on the health monitoring of concrete structures using embedded piezoelectric transducers”, *Struct. Health Monit.*, **16**(2), 202-214.
- Norris, A., Saafi, M. and Romine, P. (2008), “Temperature and moisture monitoring in concrete structures using embedded nanotechnology/microelectromechanical systems (MEMS) sensors”, *Constr. Build. Mater.*, **22**(2), 111-120.
- Qin, F., Kong, Q., Li, M., Mo, Y., Song, G. and Fan, F. (2015), “Bond slip detection of steel plate and concrete beams using smart aggregates”, *Smart Mater. Struct.*, **24**(11), 115039.
- Quenard, D. and Sallee, H. (1988), “A gamma-ray spectrometer for measurement of the water diffusivity of cementitious materials”, *MRS Online Proceedings Library Archive* **137**.
- Richardson, M.G. (2003), *Fundamentals of durable reinforced concrete*, CRC Press.
- Saare, E. and Jansson, I. (1961), *Measurement of thermal conductivity of moist porous building materials*. Proc. Internat. Assoc. of Test & Res. Lab. for Materials & Structures.
- Shukla, S., Parashar, G., Mishra, A., Misra, P., Yadav, B., Shukla, R., Bali, L. and Dubey, G. (2004), “Nano-like magnesium oxide films and its significance in optical fiber humidity sensor”, *Sensor. Actuat B: Chem.* **98**(1), 5-11.
- Song, G., Gu, H. and Mo, Y.L. (2008), “Smart aggregates: multi-functional sensors for concrete structures—a tutorial and a review”, *Smart Mater. Struct.*, **17**(3), 033001.
- Tressler, J.F., Alkoy, S. and Newnham, R.E. (1998), “Piezoelectric sensors and sensor materials”, *J. Electroceram.*, **2**(4), 257-272.
- Xu, B., Chen, H. and Xia, S. (2017), “Numerical study on the mechanism of active interfacial debonding detection for rectangular CFSTs based on wavelet packet analysis with piezoceramics”, *Mech. Syst. Signal Pr.*, **86**, 108-121.
- Yan, S., Sun, W., Song, G., Gu, H., Huo, L.S., Liu, B. and Zhang Y.G.(2009), “Health monitoring of reinforced concrete shear walls using smart aggregates”, *Smart Mater. Struct.*, **18**(4), 047001.
- Yi, T., Li, H. and Gu, M. (2011), “Optimal sensor placement for structural health monitoring based on multiple optimization strategies”, *Struct. Des. Tall Spec.*, **20**(7), 881-900.
- Yi, T., and Li, H. (2012), “Methodology developments in sensor placement for health monitoring of civil infrastructures”, *Int. J. Distrib. Sens. N.*, **8**(8), 612726.
- Yi, T., Li, H. and Gu, M. (2013a), “Recent research and applications of GPS - based monitoring technology for high - rise structures”, *Struct. Control. Health.*, **20**(5), 649-670.

- Yi, T., Li, H. and Gu, M. (2013b), "Experimental assessment of high-rate GPS receivers for deformation monitoring of bridge", *Measurement*, **46**(1), 420-432.
- Yeo, T. L., Sun, T., Grattan, K.T., Parry, D., Lade, R. and Powell, B.D. (2005), "Polymer-coated fiber Bragg grating for relative humidity sensing", *IEEE Sen. J.*, **5**(5), 1082-1089.
- Zou, D., Liu, T., Huang, Y., Zhang, F., Du, C. and Li, B. (2014), "Feasibility of water seepage monitoring in concrete with embedded smart aggregates by P-wave travel time measurement", *Smart Mater. Struct.*, **23**(6), 067003.
- Zou, D., Liu, T., Liang, C., Huang, Y., Zhang, F. and Du, C. (2015), "An experimental investigation on the health monitoring of concrete structures using piezoelectric transducers at various environmental temperatures", *J. Intel. Mat. Syst. Str.*, **26**(8), 1028-1034.
- Zou, D., Liu, T., Qiao, G., Huang, Y. and Li, B. (2014), "An experimental study on the performance of piezoceramic-based smart aggregate in water environment", *IEEE Sen. J.* **14**(4), 943-944.
- Zou, D., Liu, T., Yang, A., Zhao, Y. and Du, C. (2017), "A primary study on the performance of piezoceramic based smart aggregate under various compressive stresses", *Smart Mater. Struct.*, **26**(10), 107003.

TY